

**Table 1.** Summary of SWA-EAS design and build and ground calibration results for FM SWA-EAS heads.

Parameter	Range and resolution	EAS design goal	EAS build and calibration
Sensors		2 × EA	2 × EA
Mass	Species	Electrons	Electrons
Energy	Range	1 eV–5 keV	1 eV–5 keV
	Energy scan	64 steps	64 steps
	Resolution ( $\Delta E/E$ )	12%	13%
	Analyser constant (eV/V)	6	~6.65 (SWA-EAS1) ~6.30 (SWA-EAS2)
Angle	Range (AZ)	360°	360°
	Range (EL)	±45°	±45°
	Range scan (EL)	16 steps	16 steps
	Resolution (AZ × EL)	11.25° × 3°–8°	11.25° × 6°–12°
	Pixel FoV	11.25° × 3°–8°	11.25° × 6°–12°
Temporal	Basic accumulation period	0.96 ms	0.96 ms
	Normal mode	4 s moments	1 s moments every 4 s or 4 s moments
		100 s full 3D VDFs	1 s full 3D VDFs every 100 s (or every 400 s or every 10 s)
Burst mode	0.125 s p.a.d.	0.125 s p.a.d.	
Triggered mode	1 s full VDF every 1 s for 5 min	1 s full VDF every 1 s for 5 min	
Sensitivity	Per pixel (cm <sup>2</sup> sr eV/eV)	Variable, $\geq 8.0 \times 10^{-5}$	Variable, $8.0 \times 10^{-5}$ for pixels with clear FoV

### 3.1.6. Summary of SWA-EAS specifications at delivery

A summary of the design goals versus the achieved characteristics of the two SWA-EAS sensor heads is given in Table 1. Overall, the performance is close to that expected on the basis of the design and simulations. The energy resolution is ~13% and the two heads show only a small difference in their analyser constant,  $k$ .

The performance in elevation angle resolution has an unusual energy dependent variation. Figure 9 illustrates the elevation angle performance of the two FM sensor heads (SWA-EAS1 in left column, SWA-EAS2 in right). The top row shows the bandwidth of each of the 16 elevation settings for the sensor head (coloured traces) and the overall passband (black line). The second row then shows the response for the peak of the transmitted elevation angle distribution as a function of the voltage applied to the aperture deflection system (ratio as a function of inner hemisphere voltage). An asymmetry in the positive-negative deflection angles is observed, consistent with the charged particle optics simulations of the sensor design. The plots in the lower row show the width of the transmitted elevation angle distribution for each elevation setting (FWHM of the passbands in the upper plots). There is a variation in the acceptance angle ranging from ~6° to ~13°. This is higher than the ~2° to ~9° observed in calibrations at higher energies, typically above 1500 eV, and predicted by the simulations. Below 1500 V, the width increases from ~2° up to ~6° as the calibration energy is lowered to below 30 eV. This energy dependent behaviour is under investigation at the time of writing this paper. The most likely explanation is a broadening of the incident beam itself at lower energies. However, if the energy dependence is found to be intrinsic to the sensor response, for example, due to stray electrostatic fields not accounted for in the simulations or increased elastic scattering within the sensor apertures at low energies, this will have to be accounted for in on-board and ground calibration parameters.

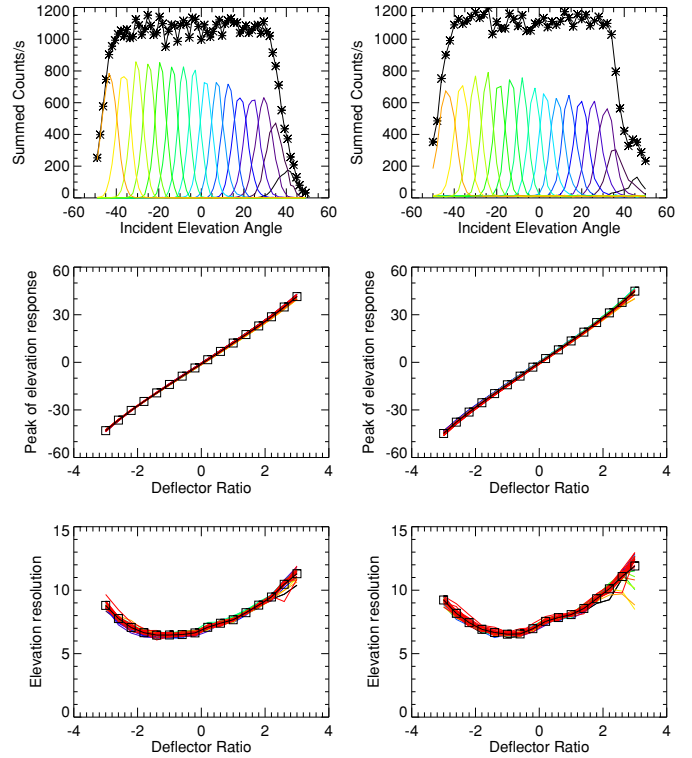


**Fig. 9.** Elevation response of FM SWA-EAS sensors heads (SWA-EAS1 in left column, SWA-EAS2 in right column). *Top row:* counts received in each sensor elevation bin as a function of the elevation angle of the incident electron beam. *Second row:* elevation angle showing peak response as a function of the voltage ratio applied to the deflectors, showing good linearity. *Bottom row:* FWHM of the response angle as a function of the voltage ratio, indicating that there is an asymmetry in the response for “upward” and “downward” sweeps and that the acceptance angle is larger at larger deflections.

Overall, the SWA-EAS sensor will be capable of measuring the full 3D VDF of electrons in the energy range 1 eV–5 keV with a cadence of 1 s, with measurements of a 2D pitch angle sample at 0.125 s cadence. This covers the core, halo, and strahl components of the overall solar wind electron population with high resolutions in time, energy, and angular acceptance. Due to telemetry restrictions, these data must be processed on board to form moments of the electron distribution which will be added to the telemetry stream every 4 s, or returned in their raw form only sporadically. Full 3D VDFs will be routinely returned at a nominal cadence of 100 s, but can also be returned at faster or slower rates depending on the telemetry constraints. Full-time resolution 3D VDFs will also be returned in short (~5 min) periods following occasional response to a triggered event (Walsh et al. 2020). The 2D pitch angle data will also be returned from short (5–10 min) periods of burst mode activation.

## 3.2. The SWA Heavy Ion Sensor (SWA-HIS)

### 3.2.1. SWA-HIS introduction

In support of the Solar Orbiter mission science goals, SWA-HIS will measure heavy ion composition and kinetic properties from solar wind up through suprathermal energies. To achieve these science goals, SWA-HIS must address two fundamentally different sets of measurement objectives. First, it must measure the ion and elemental composition and 3D VDFs of heavy ions (He–Fe) in the bulk solar wind between 0.5 and 18 keV/e.

Second, it must measure the ion and elemental composition and 3D VDFs of the major constituents: He, C, O, and Fe in the suprathermal energy range up to 60 keV/e. To achieve the characterisation of 3D VDFs for these populations, SWA-HIS is mounted within a cut-out in the corner of the spacecraft heat shield, with its FoV facing the solar direction. It has a FoV that spans a native  $96^\circ$  in the ecliptic from  $-30^\circ$  off the Sun-Spacecraft line to  $+66^\circ$  off the Sun-spacecraft line to account for the aberration of the solar wind due to motion of the spacecraft, and to allow for improved sampling of suprathermal and pickup ions. SWA-HIS scans through  $\pm 17^\circ$  above and below the ecliptic. SWA-HIS will measure alpha particle and heavy ion 3D VDFs in solar wind, pickup ion, and suprathermal energy ranges, with native time resolution as high as 4 s in Burst Mode, 30 s in Normal Mode, and 300 s for Normal Mode (Low Cadence). This time resolution corresponds to the time it takes to scan the entire energy range from 0.5–80 keV/e in 64 steps, and sample all elevation angles in 16 steps. SWA-HIS will return a number of heavy ion rates, onboard calculated VDFs, and a statistically representative sampling of Pulse Height Analysis (PHA) event words to reconstruct high fidelity 3D VDFs of all heavy ions. From these 3D VDFs, SWA-HIS will provide measurements of elemental abundances and charge state distributions of He, C, O, Mg, Si, and Fe. SWA-HIS will provide the first-ever solar wind and suprathermal heavy ion composition measurements in the inner heliosphere.

### 3.2.2. SWA-HIS design overview

Figure 10 shows a photograph (left) and computer-aided design (CAD) model (right) showing a complete overview of the mechanical sections of SWA-HIS. Due to its exposure to the Sun, SWA-HIS includes its own heat shield, which wraps around the entrance system, as seen in the photograph. The aperture of the instrument is a narrow slit in the instrument heat shield, behind which the SWA-HIS pairs an electrostatic analyser (EA) with entry ion steering (IS) to form (right-upper) the upper EA-IS subsystem, which will optimise the out-of-ecliptic particle sampling. The bottom of the EA-IS is mated to a grounded housing (right middle) containing an isolated time of flight (TOF) telescope and associated electronics. The heat shield, EA-IS, and grounded housing containing the TOF telescope are mounted on top of the main electronics (ME) box (right-lower), which contains the low-voltage power supply (LVPS), post-acceleration (PA) high-voltage power supply (HVPS), and associated boards.

**SWA-HIS EA-IS system.** The SWA-HIS entrance system is comprised of a top-hat hemispherical EA paired with IS plates behind the entrance aperture in the instrument heat shield. The ion steering plates include top and bottom deflectors as well as a “top-cap” deflector; these deflectors steer ions in through the entrance aperture from above and below the ecliptic. Ions can be steered  $\pm 17^\circ$  in the polar direction, above and below the aperture.

**HIS TOF telescope.** The TOF telescope measures time-of-flight and total kinetic energy of incoming ions. When paired with the EA-IS, this provides optimum separation of incoming ions by energy, mass, and charge. The TOF telescope is floated at  $-25$  keV, supplied by the PA HVPS, which is housed in the ME box. The TOF telescope is isolated from the grounded housing by the PA vacuum gap shown in Fig. 10 (right). The TOF telescope also includes a carbon foil (CF) entrance window, MCPs paired with position sensing readout anodes, and an array of solid state detectors (SSDs), and all of the associated electronics.

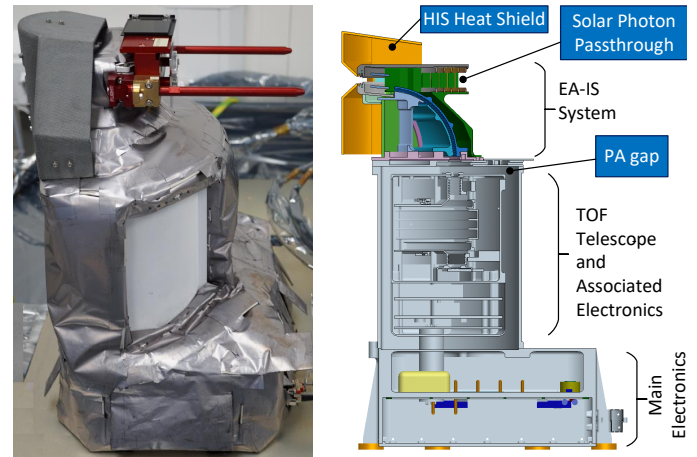


**Fig. 10.** *Left:* photograph of SWA-HIS in “as delivered” configuration. *Right:* schematic showing the different SWA-HIS building blocks.

The isolated detector section (DS) data interface is located in the TOF telescope.

**HIS ME box.** The ME box includes the PA-HVPS, the detector section LVPS, the ground side of the data interface with the TOF telescope, the EA-IS HVPS, the C&DH board, and the instrument LVPS. The C&DH board runs the flight software, which controls most aspects of the sensor.

### 3.2.3. SWA-HIS measurement principle

SWA-HIS requirements demand the derivation of five key properties from the measurements of all ions: mass ( $m$ ), charge ( $q$ ), speed ( $v$ ), and direction of incidence, elevation ( $\theta$ ) (above and below aperture, in the polar direction), and azimuth ( $\phi$ ) (along the entrance aperture, nominally in the ecliptic). SWA-HIS provides these properties as follows: SWA-HIS EA-IS provides  $E/q$  and  $\theta$  information. SWA-HIS TOF provides the  $\phi$  information through both the SSD ID, and through the imaging of secondary electrons on the Start MCP anode, generated as the ion passes through a thin carbon foil at the entrance of the TOF telescope. These secondary electrons also serve to start the timing window for TOF ( $\tau$ ) measurement when they impact the Start MCP. To push solar wind ions above the SSD energy threshold, the TOF telescope floats at a potential of  $-25$  keV. This potential accelerates the incoming solar wind ions so that their detection efficiencies are almost independent of their initial speed. Once the ion impacts the SSD, secondary electrons are emitted and steered to the Stop MCP for closure of the timing window, from which the speed of the ion within the TOF chamber can be determined. The SSD measures the total energy of the accelerated ion ( $E_{\text{Tot}}$ ). Combining  $E/q$ ,  $\tau$ , and  $E_{\text{Tot}}$  enable the calculation of ion’s mass, charge, and velocity (e.g. Shearer et al. 2014). Angles of incidence are obtained as described above. This completes the five independent measurements required for unique ion identification and characterisation.

The conceptual design of the SWA-HIS EA-IS is driven by requirements that major heavy ion species should be measured up to energies of 60 keV/e ( $\Delta E/E \leq 10\%$ ), and a maximum time resolution of 4 s for alpha particles and 30 s for heavy ions. The FoV of the instrument ranges from  $-33^\circ$  to  $+66^\circ$  in the azimuthal (ecliptic plane), and  $\pm 17^\circ$  in the polar directions for optimum sampling of the solar wind ions, pickup ions, and suprathermal

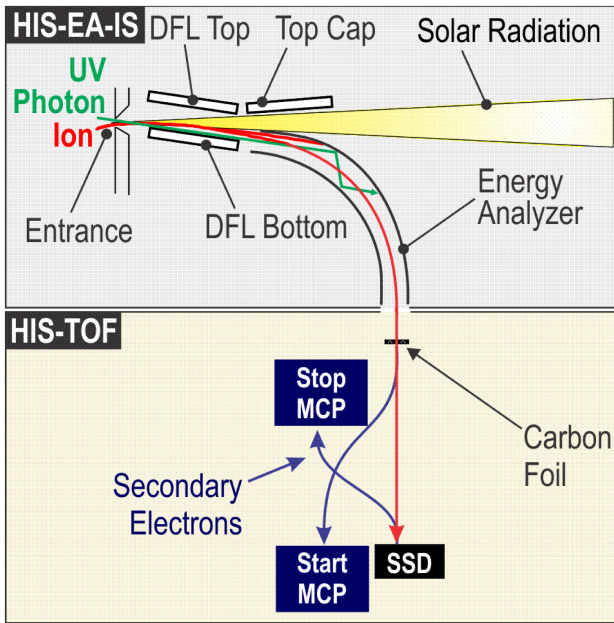


**Fig. 11.** Schematic of SWA-HIS with example particle trajectory. The cut-plane for the top part of the figure is that containing the Sun-spacecraft line and the direction of elevation deflection. The yellow shading represents the passage of direct solar light through the sensor and the red curve indicates a representative ion trajectory in this plane. The instrument has partial cylindrical symmetry extending from  $-33^\circ$  to  $+66^\circ$  out of the plane of the figure.

ions. The pixel resolution is  $\sim 6^\circ \times 6^\circ$ , which corresponds to a FoV comprising 16 azimuth and six polar sectors.

Figure 11 shows the two SWA-HIS ion optics subsystems: (1) The EA-IS is designed to achieve the required FoV and energy per charge ( $E/q$ ) selection. An opening in the rear side of the EA-IS allows solar radiation to pass through unhindered. (2) The TOF telescope contains start and stop MCPs for time of flight measurement ( $\tau$ ) and SSDs for total ion energy ( $E_{\text{Tot}}$ ) measurements. A carbon foil covers the optical path entrance to the TOF telescope as serves as a source of secondary electron to start the timing window.

Solar wind ions that enter the small aperture are steered by the IS into the EA. The EA voltage settings allow selection of ions within the appropriate  $E/q$  range to be transmitted into the TOF telescope. The IS plates, comprised of a deflector top plate (DFL Top), deflector bottom plate (DFL Bottom), and a “top-cap” serve plate to steer in ions over the range of  $\pm 17^\circ$  in the polar direction. The EA-IS system is swept through voltages to scan the full elevation angle range and the full  $E/q$  range once per scan. Stray light and any ions outside this  $E/q$  range are suppressed by surface coatings and scalloping of the EA. The energy resolution of the EA is 6–10% and the elevation angle resolution is  $< 3.5^\circ$  and have been verified by both ion optics simulations and laboratory calibration. The EA subsystem has a sufficiently large geometric factor ( $\sim 2 \times 10^{-5} \text{ cm}^2 \text{ sr eV eV}^{-1}$  per  $6^\circ$  pixel) to measure 3D VDFs of Fe ions at 30 s time interval even during the lower flux and density slow solar wind conditions expected outside of 0.7 AU.

After passage through the SWA-HIS-EA and -IS subsystem, the ions converge at a focal plane that is co-aligned with the carbon foil. The entire TOF telescope, including the PA voltage gap, is designed to provide measurements  $\phi$ ,  $\tau$ ,  $E_{\text{Tot}}$ . The telescope has a simple interface to the SWA-HIS-EA subsystem via an aperture at ground potential. After passing through the

vacuum gap, which provides a stand-off distance sufficient for safe operation at the highest voltages, an accelerated ion penetrates a segmented ultra-thin ( $\sim 0.9\text{--}1.1 \mu\text{g cm}^{-2}$ ) carbon foil and emits secondary electrons. These secondary electrons are deflected onto a Start MCP while maintaining their azimuthal location. The impact of secondary electrons on the Start MCP generates a start signal for TOF analysis. The ion continues through a nearly field-free volume before hitting the SSD array and emitting another set of secondary electrons that are deflected onto a Stop MCP. The electron impact generates a stop signal to complete the TOF ( $\tau$ ) measurement. A specially tailored electrode is situated between the start and stop MCPs to eliminate ion feedback between the two. The SSD array is comprised of 30 pixels spanning  $96^\circ$  in azimuth. Each pixel is comprised of a fully-depleted thin-window silicon detector with  $500 \mu\text{m}$  depletion depth and  $< 50 \text{ nm}$  dead-layer thickness. The pixel shape is a trapezoidal approximation to an arc segment, with an average width of 4.8 mm, a radial length of 3.7 mm, and an azimuthal width of  $3^\circ$ . The  $96^\circ$  azimuthal span will cover the required FoV and also accommodate azimuthal scattering from heavy ions as they pass through the carbon foil. The angle, TOF, and energy resolutions of the TOF-SSD subsystem are sufficient to meet all of the Solar Orbiter science objectives for SWA-HIS.

### 3.2.4. SWA-HIS design details

Figure 12 shows the SWA-HIS block diagram, indicating the functional grouping of the subsystems shown in Fig. 10. The figure includes all the PCBs contained in each subsystem, as described below.

**HIS EA-IS subsystem.** The EA-IS subsystem and supporting electronics were built by Institut de Recherche en Astrophysique et Planétologie (IRAP), in Toulouse, France. With the exception of the geometric factor, it is nearly the same design as the SWA-PAS electrostatic analyser. As SWA-PAS uses channeltron detectors, the SWA-HIS EA-IS geometric factor is  $\sim 1/3$  smaller to accommodate the required MCP lifetime. The EA-IS system sits behind the carbon-carbon instrument heat shield and includes a rear exit for solar photon pass-through. The EA-IS is physically mounted to the outer housing of the SWA-HIS DS. The EA-IS body is grounded with a grounding strap to this same outer housing. Ions enter the instrument through a 3.5 mm slit in the SWA-HIS EA-IS; their elevation angle is controlled by top and bottom IS plates, with maximum voltages of  $\pm 5.6 \text{ keV}$ . The EA has a central radius of 70 mm with 2.3 mm hemisphere spacing and maximum voltage of  $\pm 5.5 \text{ keV}$ . The EA-IS entrance has knife edges to define the opening. The curved EA plates are scalloped and surface coated for light baffling. Electrical connections from the EA-IS run via cables down the outside of the TOF telescope and around the top of the ME box before mating up to the EA-IS HVPS inside the ME box. The EA-IS HVPS can be commanded into a sweeping mode where the voltages stored in the EA-IS table are stepped through with the timing specified in the table; static voltages were used during ground testing. Commanded parameters are monitored via flight software and the analogue readback of the direct voltage when sampled. The EA-IS stepping is fully synchronised with the TOF and energy data taken by the sensor via hardware handshakes across the optical link.

**HIS detector section and readout electronics subsystem.** The TOF telescope and associated electronics are isolated from the grounded housing that encloses them and separated from the housing by the PA gap. This gap is sized to keep electric

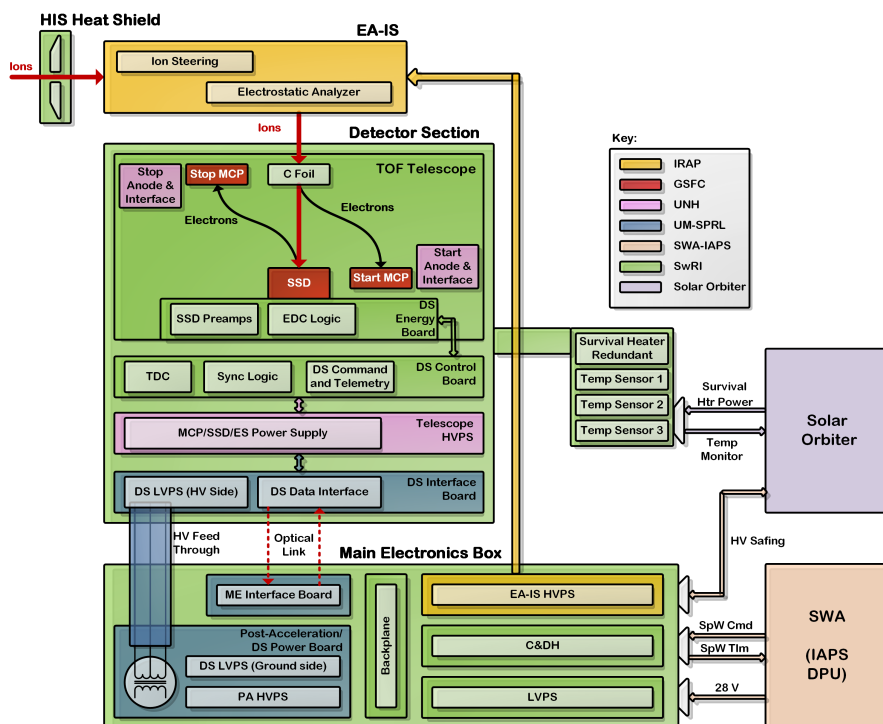


Fig. 12. HIS block diagram.

fields low according to Pachen's law in order to prevent voltage breakdown. The nominal  $-25$  keV potential, supplied by the PA HVPS, is applied to the entire TOF telescope, accelerating ions entering from the EA-IS by  $25$  keV/e. The SWA-HIS TOF telescope and supporting electronics were built in the USA by a consortium comprising Southwest Research Institute (SwRI), University of Michigan (UMich), University of New Hampshire (UNH), and NASA GSFC. The interface between the EA-IS and DS subsystems is straightforward and controlled by an interface control document (ICD). This interface is an aperture at ground potential. The TOF telescope includes SSDs, MCPs, and associated electronics, control boards, and power supplies.

The ion entrance into the TOF telescope is fitted with a carbon foil and support grid. The ion path-length from the carbon foil to the SSD surface is  $9$  cm. The MCP Start and Stop stacks are made of two plates each in a classic chevron configuration with the front-side biased and the back side near-ground. The MCPs are mechanically clamped with tension springs and electrode contacts within the stack. Voltages are optimised for MCP throughput and vary with age, but are nominally set to  $2.1$  keV across the plate stacks. MCP gain is adjustable by increasing or decreasing the MCP bias voltage as needed and is anticipated to change over the mission lifetime. Azimuthal position can be obtained from the start position anode. The angular resolution is determined by the delay line with  $2^\circ$  strips. The TOF resolution, derived from the MCP signals, is  $<1.7$  ns, with a TOF bin size of  $0.64$  ns. The TOF resolution is species and energy dependent and has been calibrated in the laboratory. Cross talk between Start and Stop MCP is virtually eliminated by a set of dedicated electrodes. The detector section's TOF and position measurements design was optimised with 3-dimensional electrostatic simulations (using SIMION<sup>1</sup>) and hundreds of hours of ion testing on the detector section prototype. Additionally, ion feedback at both the Start and Stop MCPs is minimised by ensuring the bias angle on the exit plate is at least  $15^\circ$  to the normal of the anode and

applying only  $50$  V between the exit of the plate and the anode itself. Each SSD comprises one pixel, with  $30$  pixels mounted on ceramic carriers spanning the azimuthal FoV. Angular resolution of  $5^\circ$  is limited by the size of the pixels and the required electronics for each pixel.

The isolated TOF electronics are floated at the same potential as the TOF telescope. These DS electronics include the detector section interface board (DSIB), the MCP HVPS, the DS control board (DSCB), and the DS energy board (DSEB). The DSIB supplies the low voltages for the DS (derived from the AC voltage riding on the PA-HVPS signal) and the DS side of the optical data communications link to the ME box. The MCP HVPS provides float and bias voltages for both the start and stop MCPs as well as the SSD bias voltage. All outputs are programmable. The DSCB uses an FPGA to perform the TOF measurement, time-to-digital conversion (TDC), application of commandable event logic, and combination of these signals with the energy measurement to form a partial PHA event word. DSCB event logic can be configured to trigger on events that have measurements of SSD energy only, TOF only, or both. The DSCB then sends events to the DSIB for transmission to the ME through the optical data communications link and provides fault detection, isolation and recovery (FDIR) capabilities. The DSEB houses the SSDs and collects and processes signals from the SSDs, using a specially designed,  $32$  channel ASIC. The DS also holds the HV side of an LVPS for powering these DS electronics. Measurement data are transmitted to the ME at ground potential via an optical link on the DSIB. The bulk of this data are PHA event words, containing the measurements of TOF ( $9$  bits), total energy ( $9$  bits), azimuthal angle ( $6$  bits), SSD ID ( $5$  bits), decimation class ( $3$  bits) and multi-SSD flag ( $1$  bit). These bits are streamed across the optical link and paired with the rest of their measurement information (e.g.  $E/q$  step, elevation angle) in the ME.

*HIS main electronics.* The ME sit below the TOF system at spacecraft potential. The ME includes: the LVPS, the Command and Data Handling Board (C&DH), the EA-IS HVPS, the optical link, and the PA-HVPS. The LVPS supplies all of the low

<sup>1</sup> <https://simion.com/docs/simion8brochure.pdf>

voltages to the other ME boards, as well as a 20 V<sub>pp</sub> (peak-to-peak) square wave AC supply to link low voltages to the detector section. The C&DH board controls the balance of the instrument and houses the memory, processor and flight software, as well as FDIR functions. The EA-IS HVPS, built by IRAP, drives the EA-IS voltages. This HVPS consists of a pair of commandable bulk-supplies and commandable outputs for each of the electrodes in the EA-IS system. The optical link provides the ME side of the system for digital communication to the DS. The PA-HVPS provides the floating voltage to the detector section as well as a pathway for low voltages to cross the post-acceleration gap. The PA-HVPS provides DC-to-DC power conversion to lift the DS to  $-25$  keV referenced to the ME ground potential. It also provides AC-to-DC conversion between the LVPS and the DS electronics. DC power is passed from the PA-HVPS across the PA gap into the detector section through a high voltage feed-through that provides both electrical isolation from ground potential and thermal isolation from the detector section. Heat generated by the AC-to-DC converter is coupled to the ME box chassis ground through a thermally conductive HV insulator.

The LVPS is free-running upon application of power with AC-link voltage commandable to on or off. Both HVPS supplies have enables and commanded output voltages. Electrical interface to the spacecraft is via a 28 V regulated, switched power line as well as a SpW data interface through the DPU. The DPU interface is limited to a SpW data link and the digital data that cross that link (i.e. heartbeats and FDIR information in addition to the normal HK and science data). The ME passes the event word to the C&DH, where the SWA-HIS flight software (FSW) completes it with the addition of the  $E/q$  (7 bits) and elevation step (4 bits) information. Each PHA word is a total of 46 bits. The C&DH board includes a SPARC-8 micro-controller (32-bit data bus) with 128 KB of external programmable read only memory (PROM), 2 MB of magnetic random access memory (MRAM) and 16 MB of static random access memory (SRAM). The ME also include temperature sensors and survival heaters. Radiation shielding in the ME is provided by the aluminium enclosure.

The SWA-HIS FSW controls the instrument primarily through the science programme, which is separated into several tasks. The “main” task runs at 10 Hz and performs processes such as receiving and validating commands, building and sending HK-related telemetry packets, running macros, sweeping EA-IS HV, and monitoring safety limits. The “science” task handles the fairly complex processing required to meet SWA-HIS science requirements, such as collecting PHA words and sorting them into bins subdivided by priority, counting them into priority rate and on-board VDF histograms, and randomly selecting them for inclusion in telemetry. SWA-HIS was designed to handle events at rates of up to 100 kHz, including both the hardware and software aspects of the PHA processing pipeline. Many features are table-based to allow for easier reconfiguration, including many EA-IS parameters (e.g. voltage steps, dwell & settling times), PHA handling parameters (e.g. E-TOF boxes for each priority range and  $E/q$ , sizes of buffers and number of PHA words per energy scan), and data product specifics (e.g. sizes and ions chosen for on-board VDFs). It also handles data compression, memory operations and scrubbing.

### 3.2.5. SWA-HIS testing, characterisation and calibration

SWA-HIS has been characterised at both subsystem and instrument levels, with subsystem testing taking place at UMich, SwRI, UNH, GFSC, and IRAP. SWA-HIS has been calibrated at the instrument level at three different facilities, during four test sessions, as summarised in Table 2.

**Table 2.** SWA-HIS ground calibration programme.

	Location	Dates	Configuration	Scope of calibration
1	H30 at SwRI	Sep–Oct 2015 and Jan–Mar 2016	EA-IS	Optimisation of the EA-IS voltages
2	H19 at SwRI	Sep–Nov 2016	Complete sensor minus EA-IS	Mass (1–56) and energy (0.1–450 keV) response
3	Mefisto at Bern	Jan–Feb 2017	Complete sensor	Charge (1–4), mass (1–84) and energy/charge (3–60 keV/e) response
4	H19 at SwRI	Mar–Apr 2017	Complete sensor	Geometric factor

Test session 1 involved testing the EA-IS subsystem at SwRI. Testing lasted 36 days where the EA-IS was combined with a mock-up TOF section with a phosphorus screen in the SSD plane. Particle interactions with the phosphorus screen were imaged with a camera. This setup did not allow for TOF measurement, but was dedicated to evaluating the electro-optics and ion trajectories, with full post-acceleration. The ion beam consisted of Ar<sup>+</sup> with energies ranging from 1 keV to 40 keV. Illumination of the EA-IS aperture was completed with a broad, uniform, parallel beam larger than EA-IS aperture. During this test, the EA-IS and mock-up TOF were powered by laboratory equipment.

Calibration of the EA-IS addressed a number of aspects of performance. These included determination of: Energy-angle response of EAIS; optimal tuning of the EAIS voltages; elevation and azimuth response; energy-per-charge resolution; elevation angle resolution; ion optics and ion focus onto SSD; and relative efficiency.

Test session 2 was completed at SwRI with only the TOF telescope and associated electronics. It consisted of 5 days of beam testing without post-acceleration and 4 days of testing with full post-acceleration of the ion beam. The TOF telescope was subjected to a beam of H<sup>+</sup>, H<sub>2</sub><sup>+</sup>, He<sup>+</sup>, N<sup>+</sup>, H<sub>2</sub>O<sup>+</sup>, Ne<sup>+</sup>, Mg<sup>+</sup>, N<sub>2</sub><sup>+</sup>, Ar<sup>+</sup>, Ar<sup>2+</sup>, Ar<sup>3+</sup>, and Fe<sup>+</sup>. Beam energies ranged from 0.3 keV to 450 keV (1.35 MeV for Ar<sup>3+</sup>), with beam intensities in the kHz range. The ion beam was vignettted by a 3 mm dia hole (7 mm<sup>2</sup>) to simulated a pencil beam incident on the TOF aperture. Flat ion beam illumination of the TOF aperture was also conducted. During 80 h of operations there were no spurious events detected.

Test session 3 was completed in the Mefisto vacuum chamber at the University of Bern with the full integrated sensor. Testing lasted 21 days and was conducted with all voltages operating at nominal flight-like settings. The instrument was subjected to a beam of H, H<sub>2</sub>, He, C, N, O, F, S, Ar, Ca. Beam energies ranged from 3 keV to 60 keV, with beam intensities in the kHz range. A vignettted beam through a 2 mm diameter hole illuminated the instrument aperture. The testing included over 200 h of operations with no spurious events record.

Test session 4 was conducted at SwRI and included 5 days of testing of the integrated instrument with full PA voltages applied. The instrument was subjected to a beam of H, He, and N. Beam energies ranged from 0.3 keV to 60 keV, with beam intensities in the kHz range. The instrument aperture was illuminated with a flat beam. In over 80 h of operations no spurious events were recorded.

Overall, during test sessions 2–4, a number of aspects of sensor performance were assessed. These included the following: aliveness of the sensor; communication at various speeds;